Enhanced removal of Cd(II) and As(III) from waters using S-Fe-C composites: Performance and mechanisms

Zihao Liang[1,2], and *Gongning* Chen[1,2,*]

[1]College of Environmental Science and Engineering, Guilin University of Technology, Guilin, 541004, China
[2]Guangxi Key Laboratory of Environmental Pollution Control Theory and Technology, Guilin University of Technology, Guilin, 541004, China

Abstract. Protecting ecosystems and human health from potentially toxic elements (PTEs) like Cd(II) and As is critical. The results showed that S-nZVI particles were uniformly dispersed in biocarbon matrix. The pseudo-second-order kinetics and Langmuir model can better match the adsorption process of Cd(II) and As(III) by SFC., with the maximum removal capacity of 405 $mg \cdot g^{-1}$ and 349 $mg \cdot g^{-1}$, respectively. Biochar enhances electron transport and prevents S-nZVI agglomeration. The removal mechanisms of SFC, including chemical precipitation, ion exchange and oxidation, shows great potential for remediation of PTEs pollution in irrigation water.

1 Introduction

Due to the strong toxicity of cadmium(Cd(II)) and arsenic(As), there is a growing concern that irrigation water is contaminated by Cd(II) and As(III) from various industrial activities [1–3]. These contaminants build up in the food chain and can cause serious health problems such renal failure, bone demineralization, and cancer [4,5]. Several techniques have been proposed to remove Cd(II) and As(III) from water, but all have faced problems such as high cost or poor effectiveness[6–8]. Adsorption is an effective strategy due to its cost-effectiveness and in situ application. Biochar has become a research hotspot in the field of effective toxic element scavengers due to its various excellent properties such as high porosity, large specific surface area, and diverse surface functional groups[9,10]. However, pristine biochar has limited affinity for cadmium and arsenic, necessitating modification to enhance its adsorption capacity. Nano zero-valent iron is an iron material with a substantial surface area and reactivity characterized by iron oxide as the shell layer and Fe^0 as the core, which can be used to immobilize PTEs in water and soil. Stabilizing nZVI with porous materials like biochar enhances its stability and efficiency in removing contaminants. Sulfide-modified nZVI (S-nZVI) exhibits higher reactivity and better dispersibility[11–13]. At present, the composite materials used for adsorption generally have a small adsorption capacity for heavy metal ions, which can not efficiently and thoroughly adsorb the target

*Corresponding author: 790413605@qq.com

pollutants. Secondly, most of the composite adsorbents are difficult to be recovered after entering the water or soil, which may also cause potential secondary pollution risks to the environment. The development of composite materials combining biochar and S-nZVI offers hope for the efficient and reusable removal of heavy metals [14,15]. This study aimed to: (1) synthesize and characterize SFC for removing PTEs from waters; (2) analyze its physicochemical properties and structure; (3) evaluate its removal performance and influencing factors; (4) explore the binding mechanism for Cd(II) and As(III); and (5) evaluate its effectiveness in eliminating contaminants from real natural irrigation water.

2 Methods and experiments

Using bagasse as raw material, bagasse biochar was prepared by pyrolysis at 500℃ for 2 hours, and KBC was prepared by KOH treatment and pyrolysis at 800℃ for 2 hours. The SFC was prepared by combining KBC with $FeCl_2$, $NaBH_4$, and $Na_2S_2O_4$. The SFC are centrifuged under N_2 protection and stored in anhydrous ethanol. Langmuir and Freundlich models were used to fit the adsorption effect of the material, and the adsorption mechanism was verified. The effects of the coexistence of anions and humic acid on the simultaneous removal of Cd(II) and As(III) were also investigated, and the application potential of SFC was confirmed in actual irrigation water samples.

3 Results and discussion

3.1 Characterization

The morphological and structural characteristics of SFC were characterized by SEM images and various characterization techniques (Figure 1). The results show that BC has abundant pore structure and large specific surface area, which is suitable for S-nZVI carrier. S-nZVI exists in the form of nanosheet layers and is easy to agglomerate, while SFC improves the stability of S-nZVI and reduces the agglomerate phenomenon by using BC as a supporting framework. The pores of SFC composite are mainly medium pores (9.24nm) with a specific surface area of 240.1 $m^2 \cdot g^{-1}$, indicating that the stability of S-nZVI can be effectively enhanced by using BC with a porous structure as the carrier. XRD analysis showed the presence of FeS phase in SFC and S-nZVI, indicating that iron sulfide was successfully loaded on the biochar. FTIR spectra identify key functional groups in BC, including C-O-C and O-H, indicating that oxygen-containing functional groups in BC are effective adsorption sites for metal ions, which is conducive to the interaction with S-nZVI.

3.2 Kinetic and isotherm

Studies have shown that iron sulfide composites (SFC) are superior to sulfide nano zero-valent iron (S-nZVI) and bagasse biochar (BC) in the removal of Cd(II) and As(III) (Figure 2). The pseudo-second-order kinetic model accurately describes the adsorption process of SFC, indicating that chemisorption is the main mechanism. The adsorption rate constant of SFC is higher than that of S-nZVI and BC, indicating that SFC has higher adsorption capacity, which is related to more active sites and excellent diffusion rate. Adsorption isotherm analysis showed that the maximum removal rates of Cd(II) and As(III) by SFC were significantly higher than those of BC and S-nZVI, and better than other similar materials (Table 1).

3.3 Effect of water chemistry

In real wastewater and irrigation waters, Cd(II) removal by SFC is hindered by Ca^{2+}, Mg^{2+}, and K^{+} ions due to competition for adsorption sites, with Mg^{2+} causing the most significant reduction, while PO_4^{3-} significantly enhances Cd(II) removal by 26.8% through cadmium phosphate formation. Conversely, PO_4^{3-} inhibits As(III) adsorption, reducing removal rates for BC, S-nZVI, and SFC by 25.6%, 18.0%, and 1%, respectively. Ca^{2+}, Mg^{2+}, and K^{+} improve As(III) removal by increasing the material's surface charge and promoting Fenton-like reactions that oxidize As(III) to As(V), forming $H_2AsO_4^{-}$ which is more easily adsorbed. Additionally, SFC slightly increases solution pH, enhancing As(III) ionization and adsorption affinity (Figure 3).

Table 1. Comparison of adsorption capacity of Cd(II) and As(III) by the different adsorbents.

Raw materials	pH	Adsorption capacity of Cd(II) ($mg \cdot g^{-1}$)	Adsorption capacity of As(III) ($mg \cdot g^{-1}$)	References
Zeolite-nZVI	7.0	48.63	11.52	[16]
GB-nZVI	7.0	46.4	181.5	[17]
S-nZVI	7.0	11.37	230.29	[18]
biochar supported S-nZVI	5.0	162	276	[19]
α-FeOOH modified wheat straw biochar	4.0	62.9	78.3	[20]
Biochar-supported nZVI	4.0	67.9	291	[21]
calcium-based magnetic biochar	6.0	10.07	6.37	[22]
S-Fe-C composites	4.0	405	349	This study

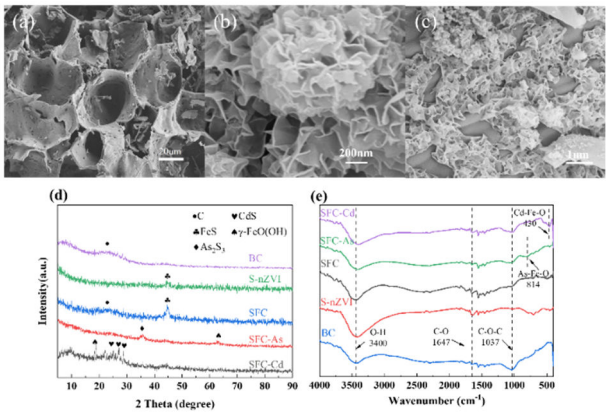

Fig. 1. SEM (a,b,c), XRD (d) and FTIR(e) of different materials.

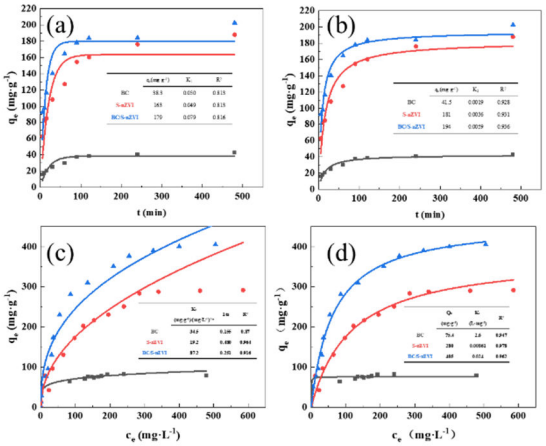

Fig. 2. Kinetic and isotherm of different materials.

3.4 Simultaneous removal of Cd(II) and As(III)

The effects of different proportions of Cd(II) and As(III) (Cd:As = 100:0, 100:100, 100:200, 200:0,200:100) on the removal of SFC were investigated (Figure 3 (c)). As the proportion increased, a synergistic effect was observed, significantly enhancing the adsorption of Cd(II). Cd(II) removal rate is the highest when the ratio of 1:1. This synergistic effect is due to the possible formation of Fe-Cd-As ternary complexes on the surface of SFC, and the absorption of As(III) ions on the surface of the material leads to an increase in negative charge, thus enhancing the adsorption of Cd(II).

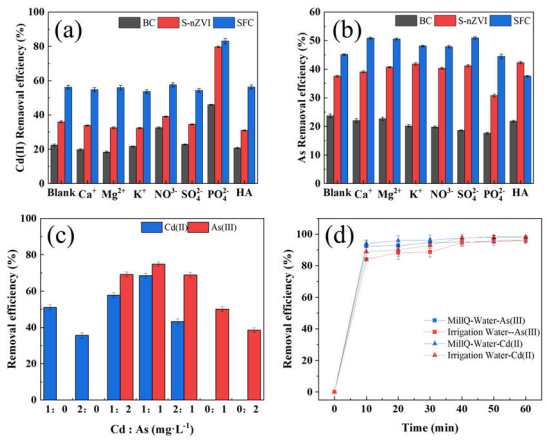

Fig. 3. Effect of SFC on the removal of Cd(II) and As(III) in water: the role of anion and humic acid (a, b), removal efficiency at different concentrations (c), and removal effect in irrigation water (d).

3.5 Application in irrigation waters

SFC can remove 98.2% of Cd(II) and 96.1% of As in actual irrigation water within 10 min, respectively, within 10 min, which was comparable to that of milli-Q water. The results show that SFC has high efficiency and anti-interference performance in purifying Cd(II) and As(III) in water (Figure 3(d)).

3.6 Mechanism

XRD analysis shows that a new diffraction peak appears after the adsorption of Cd(II) and As(III), indicating that significant oxidation occurs on the surface of SFC during the adsorption process, and precipitates of hydroxy-iron oxide and cadmium-arsenic are formed (Figure 4(a)). FTIR spectral analysis further showed that the characteristic peaks of oxygen-containing functional groups on the surface of SFC had certain shifts and intensity changes, indicating that these functional groups are related to the complexation that occurs when Cd(II) and As(III) are removed. EDS analysis showed that the distribution of Fe and O on the SFC surface was highly consistent with that of Cd(II) and As(III), and the contents of potassium and magnesium on the SFC surface were significantly reduced after the adsorption of Cd(II), indicating that SFC adsorbed Cd(II) through ion exchange mechanism[23,24]. The chemical alterations of the Cd(II) and As(III)were identified by XPS analysis (Figure 4 (b, c, d, e)). The original peaks show that S-nZVI was successfully loaded onto the BC. As(V) and As2S3 were evident in the As3d binding energy, and the production of CdS was validated by the Cd3d characteristic peak. Fe(II) and Fe0 peaks shrank after adsorption, whereas Fe(III) peaks grew, suggesting that surface iron oxidation took place. According to the Haber-Weiss mechanism, the change in the S2p peak suggests that the oxidation and precipitation of FeS happen concurrently and that the elimination of Cd(II) and As(III) is largely dependent on the chemical precipitation of sulfide (Figure 5).

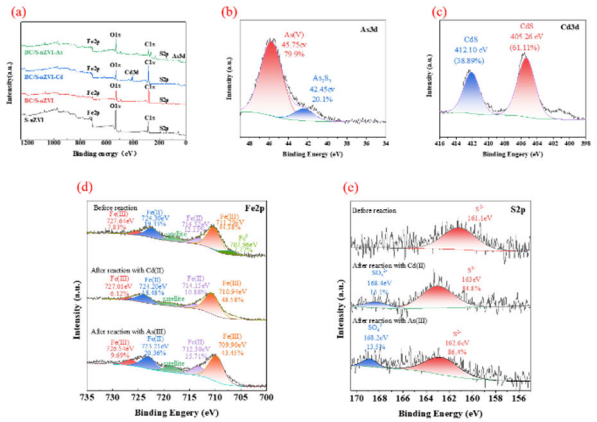

Fig. 4. XPS spectrum: Changes of surface element content and valence state of SFC before and after reaction with Cd(II) and As(III).

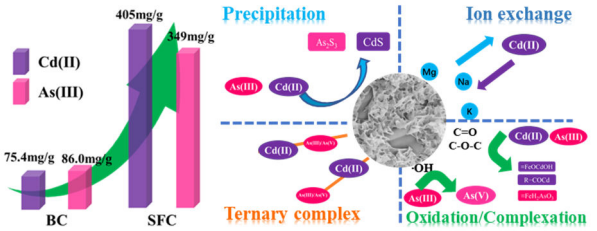

Fig. 5. Mechanism of removal of cadmium and arsenic from water by SFC.

4 Conclusion

Bagasse biochar improves the electron transfer efficiency through its high specific surface area, and supports S-nZVI through its porous structure, which reduces the agglomeration phenomenon and thus improves the removal effect of PTEs. The strong magnetic properties of SFC solve the problem of biochar recovery. Ca^{2+} and Mg^{2+} reduce the adsorption of Cd(II) by SFC, while the coexistence of As(III) in water can promote the removal of Cd(II) by SFC. The main mechanism of SFC removal of heavy metals includes oxidation, complexation, precipitation and ion exchange.

References

1. R. Sankaran, PL Show, CW Ooi, et al., Feasibility assessment of removal of heavy metals and soluble microbial products from aqueous solutions using eggshell wastes. Clean Techn Environ Policy. 2020;**22**(4):773-786. https://doi.org/10.1007/s10098-019-01792-z
2. S. Sobhanardakani, L. Tayebi, SV. Hosseini, Health risk assessment of arsenic and heavy metals (Cd, Cu, Co, Pb, and Sn) through consumption of caviar of Acipenser persicus from Southern Caspian Sea. Environ Sci Pollut Res. 2018; **25**(3): 2664-2671. https://doi.org/10.1007/s11356-017-0705-8
3. M. Xu, P. Hadi, G. Chen, G. McKay, Removal of cadmium ions from wastewater using innovative electronic waste-derived material. J. Hazard. Mater. 2014;**273**:118-123. https://doi.org/10.1016/j.jhazmat.2014.03.037
4. Q. Huang, Y. Zhang, W. Zhou et al., Amorphous molybdenum sulfide mediated EDTA with multiple active sites to boost heavy metal ions removal. CCL. 2021;**32**(9):2797-2802. https://doi.org/10.1016/j.cclet.2020.12.020
5. J. Shi, C. Guo, C. Lei et al., High-performance biochar derived from the residue of Chaga mushroom (Inonotus obliquus) for pollutants removal. Bioresour. Technol. 2022;**344**:126268. https://doi.org/10.1016/j.biortech.2021.126268
6. P. Shao, L. Ding, J. Luo et al., Lattice-Defect-Enhanced Adsorption of Arsenic on Zirconia Nanospheres: A Combined Experimental and Theoretical Study. ACS Appl. Mater. Interfaces. 2019;**11**(33):29736-29745. https://doi.org/10.1021/acsami.9b06041
7. S. Kim, KH. Chu, YAJ. Al-Hamadani et al., Removal of contaminants of emerging concern by membranes in water and wastewater: A review. Chem. Eng. J. 2018;**335**:896-914. https://doi.org/10.1016/j.cej.2017.11.044
8. S. Sobhanardakani, R. Zandipak, Synthesis and application of TiO2/SiO2/Fe3O4 nanoparticles as novel adsorbent for removal of Cd(II), Hg(II) and Ni(II) ions from water samples. Clean Techn Environ Policy. 2017;**19**(7):1913-1925. https://doi.org/10.1007/s10098-017-1374-5
9. H. Wang, X. Lou, Q. Hu, T. Sun, Adsorption of antibiotics from water by using Chinese herbal medicine residues derived biochar: Preparation and properties studies. J. Mol. Liq. 2021;**325**:114967. https://doi.org/10.1016/j.molliq.2020.114967
10. J. Qu, M. Dong, F. Bi et al., Microwave-assisted one-pot synthesis of β-cyclodextrin modified biochar for stabilization of Cd and Pb in soil. J. Clean. Prod. 2022;**346**:131165. https://doi.org/10.1016/j.jclepro.2022.131165
11. Y. Zhang, Y. Li, C. Dai, X. Zhou, W. Zhang, Sequestration of Cd(II) with nanoscale zero-valent iron (nZVI): Characterization and test in a two-stage system. Chem. Eng. J. 2014;**244**:218-226. https://doi.org/10.1016/j.cej.2014.01.061

12. B. Calderon, A. Fullana, Heavy metal release due to aging effect during zero valent iron nanoparticles remediation. Water Res. 2015;**83**:1-9. https://doi.org/10.1016/j.watres.2015.06.004
13. Y. Mu, F. Jia, Z. Ai, L. Zhang, Iron oxide shell mediated environmental remediation properties of nano zero-valent iron. Environ. Sci.: Nano. 2017;**4**(1):27-45. https://doi.org/10.1039/C6EN00398B
14. D. Lv, J. Zhou, Z. Cao et al., Mechanism and influence factors of chromium(VI) removal by sulfide-modified nanoscale zerovalent iron. Chemosphere. 2019;**224**:306-315. https://doi.org/10.1016/j.chemosphere.2019.02.109
15. H. Qie, M. Liu, D. Hou et al., The properties and efficacy of S-nZVI as a remediation agent in response to its preparation process and reaction conditions: a truth from meta-analysis. Environ. Sci.: Nano. 2023;**10**(10):2720-2732. https://doi.org/10.1039/D3EN00431G
16. Li Z, Wang L, Meng J, et al. Zeolite-supported nanoscale zero-valent iron: New findings on simultaneous adsorption of Cd(II), Pb(II), and As(III) in aqueous solution and soil. J. Hazard. Mater. 2018;**344**:1-11. https://doi.org/10.1016/j.jhazmat.2017.09.036
17. K. Liu, F. Li, J. Cui, S. Yang, L. Fan, Simultaneous removal of Cd(II) and As(III) by graphene-like biochar-supported zero-valent iron from irrigation waters under aerobic conditions: Synergistic effects and mechanisms. J. Hazard. Mater. 2020;**395**:122623. https://doi.org/10.1016/j.jhazmat.2020.122623
18. M. Ainiwaer, T. Zhang, N. Zhang et al., Synergistic removal of As(III) and Cd(II) by sepiolite-modified nanoscale zero-valent iron and a related mechanistic study. J. Environ. Manage. 2022;**319**:115658. https://doi.org/10.1016/j.jenvman.2022.115658
19. X. Zheng, Q. Wu, C. Huang et al., Synergistic effect and mechanism of Cd(II) and As(III) adsorption by biochar supported sulfide nanoscale zero-valent iron. Environ. Res. 2023;**231**:116080. https://doi.org/10.1016/j.envres.2023.116080
20. S. Zhu, T. Qu, MK. Irshad, J. Shang. Simultaneous removal of Cd(II) and As(III) from co-contaminated aqueous solution by α-FeOOH modified biochar. Biochar. 2020;**2**(1):81-92. https://doi.org/10.1007/s42773-020-00040-8
21. D. Yang, L. Wang, Z. Li et al., Simultaneous adsorption of Cd(II) and As(III) by a novel biochar-supported nanoscale zero-valent iron in aqueous systems. Sci. Total Environ. 2020;**708**:134823. https://doi.org/10.1016/j.scitotenv.2019.134823
22. J. Wu, D. Huang, X. Liu, J. Meng, C. Tang, J. Xu, Remediation of As(III) and Cd(II) co-contamination and its mechanism in aqueous systems by a novel calcium-based magnetic biochar. J. Hazard. Mater. 2018;**348**:10-19. https://doi.org/10.1016/j.jhazmat.2018.01.011
23. J. Liu, J. Jiang, Y. Meng et al., Preparation, environmental application and prospect of biochar-supported metal nanoparticles: A review. J. Hazard. Mater. 2020;**388**:122026. https://doi.org/10.1016/j.jhazmat.2020.122026
24. Y. Rashtbari, H. Arfaeinia, S. Ahmadi et al., Potential of using green adsorbent of humic acid removal from aqueous solutions: equilibrium, kinetics, thermodynamic and regeneration studies. Int. J. Environ. Anal. Chem. 2022;**102**(17):5373-5390. https://doi.org/10.1080/03067319.2020.1796993